Demagnetizing Fields in Thin Magnetic Films

By D. B. DOVE

(Manuscript received January 31, 1967)

Demagnetizing fields play an important role in the operation of many thin magnetic film devices. A requirement of high packing density leads to strong localization of induced changes in magnetization; and, therefore, to correspondingly large demagnetizing fields and drive currents. A treatment of the demagnetizing field problem for thin film materials is given here for film properties and fields which are nonuniform along the hard anisotropy axis. Specifically considered are saturating fields, variations in film thickness and anisotropy constant, interaction between films, and the effect of easy direction bias fields.

I. INTRODUCTION

The behavior of the magnetization in thin magnetic films of large lateral extent subject to a uniform applied field may be calculated directly from a knowledge of film properties and field strength. The calculation of the behavior of magnetization in the presence of nonuniformity of film properties or of applied field, however, must take into account the demagnetizing field that arises from a local nonuniformity of magnetization. Such a situation occurs in many problems of practical interest. Internally generated fields give rise to a number of effects when nonuniform fields are applied to thin uniaxially anisotropic films.[1,2] For example, the hard axis field required for saturation may be several times the anisotropy field and the induced magnetization component may spread to regions where the applied field is very small. The occurrence of such effects in thin films has been considered by Rosenberg[3] using a calculus of variations approach and by Kump and Greene[4] and Kump[5] using an iterative numerical procedure. More recently Dove and Long[6] have shown that there is a simple solution to the nonuniform field problem in the case of nonsaturating spatially periodic applied fields, and have treated localized

fields by using a Fourier series technique. Good agreement was found with Kerr-effect probe measurements on flat and cylindrical permalloy films.

The purpose of the present work is to show how the Fourier series technique permits straightforward solution of a number of thin film magnetostatic problems. Flat and cylindrical film geometries are treated; however, the results are of special interest to the case of cylindrical films with axial hard direction, owing to the circumferential flux closure. Specifically, we consider the cases of;

(*i*) nonuniform hard axis field,
(*ii*) nonuniform saturating field,
(*iii*) variation in film thickness,
(*iv*) variation in anisotropy constant,
(*v*) external fields due to magnetization distribution in film, flux linkage with conductors, magnetic shielding,
(*vi*) interaction between parallel films, keepers, and
(*vii*) nonuniform hard axis field in presence of easy direction bias field.

It is assumed that the quantities of interest vary along the film hard axis only and that properties and fields are uniform along the easy axis. Film thickness is taken to be sufficiently small that the direction of magnetization always lies in the plane of the film, exchange forces are neglected, being insignificant for cases considered, and anisotropy dispersion effects are not included.

II. GENERAL CONSIDERATIONS

We consider demagnetizing field effects that arise in thin uniaxially anisotropic films when relevant parameters vary only along the hard anisotropy axis. Many applications fall within this category and will be treated in following sections. Many of the results may be applied to thin films of other types of magnetic materials in the range where they exhibit a constant permeability, if the effective anisotropy field is taken to be equal to the saturation magnetization divided by the permeability.

Although the demagnetizing field may be found if the magnetization distribution is known, and conversely a knowledge of the field enables the distribution to be found, there is considerably greater difficulty in determining both distribution and field directly. In the thin film case, the Fourier series technique provides a means of representing the field

distribution for which the demagnetizing field can be found quite generally. The rotation of magnetization within a film may then be found by balancing, for example, (for nonsaturating fields) anisotropy torque versus the torque due to applied field and demagnetizing field. This leads to equations relating the coefficients of the various series which in a practical application may be most conveniently evaluated by computer.

The number of terms included in the series determines the resolution with which a particular curve may be delineated. However, a series with, say, 100 terms may be made to fit ordinates at 100 locations exactly, with oscillations about the required curve elsewhere. The procedure followed here is to use the series to calculate ordinates at the 100 locations, and a smooth curve is then drawn through the calculated ordinates. Refs. 7 and 8 have been found of value for the evaluation of integrals occurring in the following sections.

Numerical examples, where given, refer to nonmagnetostrictive 80/20 NiFe films. The films are finely polycrystalline and are characterized by a uniaxial anistropy. The easy direction is taken to be circumferential in the cylindrical film case.

III. NONUNIFORM HARD AXIS FIELD

This case has been discussed previously[6] but is included here briefly for completeness. Let x represent distance along the film hard direction, M is the value of saturation magnetization, T the film thickness, K the anisotropy constant and $\theta(x)$ the angle which the direction of magnetization (at x) makes with the film easy anisotropy direction. We now assume that the applied field $H(x)$ may be adequately represented over a range $-\lambda/2$ to $+\lambda/2$ by the series

$$H(x) = \sum_{n=-\infty}^{\infty} h_n \exp(2\pi i n x/\lambda) \tag{1}$$

and that the resulting hard direction component of magnetization $M(x)$ may be similarly represented,

$$M(x) = M \sum_{n=-\infty}^{\infty} m_n \exp(2\pi i n x/\lambda). \tag{2}$$

The distribution $M(x)$ gives rise to a local (positive) pole density at location (X, Y) of amount $-\text{div } \mathbf{M}(X, Y)$. This gives rise to a field $\mathbf{dH}$ at (x, y) distance R from (X, Y) given by

$$\mathbf{dH}(x, y) = -\text{div } \mathbf{M}(X, Y) \cdot \left(\frac{d\text{vol}}{R^2}\right) \cdot (\mathbf{R}) \left(\frac{1}{R}\right)$$

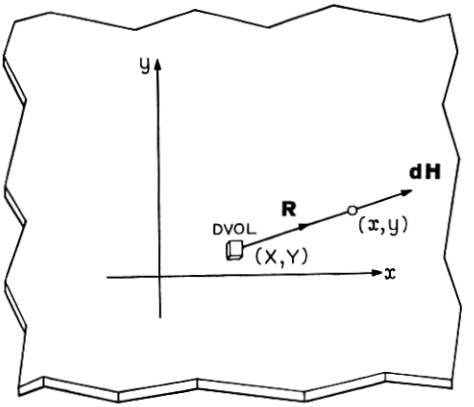

Fig. 1—A divergence of magnetization at (X,Y) gives rise to a field **dH** at (x, y). The x direction is taken to coincide with the film hard (anisotropy) direction. Under no applied field the direction of magnetization lies along the y, or easy, direction.

where **dH** is parallel to **R**, as in Fig. 1. Since the only variation of magnetization is along the x direction, variation with thickness being neglected, then div **M** reduces to $dM(X)/dx$ where $M(X)$ is the x direction component of **M**, at X.

The field **dH** has both easy and hard direction components, however, symmetry ensures that the resultant field $H_m(x)$, obtained by integrating over the film volume, lies along the hard direction. Then, we find, for a flat film

$$H_m(x) = -\int_{Y=-\infty}^{\infty}\int_{X=-\infty}^{\infty} \frac{dM(X)}{dx}\frac{(x-X)}{R^3}\,dX\,dY\,T, \tag{3}$$

where T is the film thickness. Substituting $R = [(x-X)^2 + (y-Y)^2]^{\frac{1}{2}}$ and integrating over Y we have

$$H_m(x) = -2T\int_{X=-\infty}^{\infty} \frac{dM(X)}{dx}\frac{1}{x-X}\,dX.$$

Now substituting for $M(X)$ in terms of the Fourier series, we have

$$H_m(x) = +2TM\int_{-\infty}^{\infty}\sum_{n=-\infty}^{\infty} m_n\left(\frac{2\pi in}{\lambda}\right)\frac{\exp(2\pi inX/\lambda)}{x-X}\,dX$$

and evaluating the integral,

$$H_m(x) = \sum_{-\infty}^{\infty} \alpha_n m_n \exp(2\pi inx/\lambda), \tag{4}$$

where $\alpha_n = 4\pi^2 TMn/\lambda$, $n > 0$, and $\alpha_{-n} = \alpha_n$. A similar result holds for cylindrical films having a circumferential easy direction, where x now refers to distance along the cylinder axis. In this case, we find

$$\alpha_n = 4\pi M(T/a)(2\pi na/\lambda)^2 I_0(2\pi na/\lambda)K_0(2\pi na/\lambda),$$

where a is the cylinder radius and I_0, K_0 are modified Bessel functions.

The local rotation $\theta(x)$ of magnetization away from the easy direction due to the applied field is determined by balancing the torque due to the applied field against the torques due to anisotropy and the demagnetizing field

$$2K \sin \theta(x) \cos \theta(x) + MH_m(x) \cos \theta(x) = MH(x) \cos \theta(x), \quad \text{all } x. \tag{5}$$

We note that $\sin \theta(x) = M(x)/M$, and providing $\cos \theta(x) \neq 0$, we may rewrite (5) as

$$\frac{2K}{M}\frac{M(x)}{M} + H_m(x) = H(x). \tag{6}$$

If the field is sufficiently large that $\theta(x)$ becomes equal to $\pi/2$ then the film is said to have saturated (at x) and the torque equation (5) is replaced by $M(x) = M$. In the nonsaturating case the series representations (1), (2), (4) are now substituted in (6) giving

$$H_K \sum m_n \exp(2\pi inx/\lambda) + \sum \alpha_n m_n \exp(2\pi inx/\lambda) = \sum h_n \exp(2\pi inx/\lambda),$$

where $H_K = 2K/M$. Equating coefficients of corresponding terms gives the result,

$$m_n = h_n/(H_K + \alpha_n).$$

Hence, the series for the $M(x)$ distribution may be obtained in terms of the coefficients of the applied field and geometrical parameters α_n which automatically take into account the demagnetizing field,

$$M(x) = M \sum_{-\infty}^{\infty} \frac{h_n}{H_K + \alpha_n} \exp(2\pi inx/\lambda). \tag{7}$$

As an example, we consider a wire at distance d from a flat film, lying parallel to the film easy direction. A current I along the wire produces a hard direction field component given by $H(x) = CdI/(d^2+x^2)$, where the origin for x is taken directly beneath the wire, and C is a calibration constant whose value depends on the units used, ($C = 78.8$ for d and x in mil inches, I in amperes, H in oersteds). It is

next assumed that the field is repeated at intervals λ along the hard direction in such a way that the field over one wavelength is given by

$$H(x) = \frac{C\,dI}{d^2 + x^2}, \qquad -\frac{\lambda}{2} \leqq x \leqq \frac{\lambda}{2}.$$

To determine the Fourier coefficients we proceed in the usual way, and find that for λ sufficiently large $H(x)$ is given to a good approximation by the cosine series,

$$H(x) = \frac{CI\pi}{\lambda} + \frac{2CI\pi}{\lambda} \sum_{n=1}^{\infty} e^{-2\pi nd/\lambda} \cos 2\pi nx/\lambda.$$

Substituting into (7) we have

$$M(x) = \frac{CIM\pi}{\lambda H_K} + \frac{2CIM\pi}{\lambda} \sum_{n=1}^{\infty} \frac{e^{-2\pi nd/\lambda}}{H_K + \alpha_n} \cos 2\pi nx/\lambda. \tag{8a}$$

If such a drive wire arrangement is used to apply a field to a cylindrical film, there is some variation in axial field strength across the cylinder. In many cases of interest, the cylinder diameter is small compared with axial dimensions and there is very tight magnetostatic coupling around the circumference. We therefore take the effective axial field as that applied along the wire axis, a reasonable approximation for many cases. The result (8a) then applies to the cylindrical film case provided α_n is given the appropriate value.

When a field is applied by a circular loop of radius d around the film (of radius a), it may be shown that the axial field at the surface is given by the series, for λ sufficiently large,

$$H(x, a) = \frac{CI\pi}{\lambda} + \frac{2CI\pi}{\lambda} \sum_{n=1}^{\infty} \frac{2\pi nd}{\lambda} K_1\left(\frac{2\pi nd}{\lambda}\right) I_0\left(\frac{2\pi na}{\lambda}\right) \cos \frac{2\pi nx}{\lambda},$$

where K_1, I_0 are modified Bessel functions. The field is defined over $-\lambda/2$ to $+\lambda/2$ and $d > a$. The axial component of magnetization in a cylinder excited by such a field is then,

$$M(x) = \frac{CIM\pi}{\lambda H_K} + \frac{2CIM\pi}{\lambda} \sum_{n=1}^{\infty} \frac{\frac{2\pi nd}{\lambda} K_1\left(\frac{2\pi nd}{\lambda}\right) I_0\left(\frac{2\pi na}{\lambda}\right) \cos \frac{2\pi nx}{\lambda}}{H_K + \alpha_n}. \tag{8b}$$

Similar results may be derived for fields applied by more complicated drive wire or drive strap arrangements. It can be noted that the effect of superimposing several applied fields results simply in superimposing the magnetization distributions obtained for the fields separately. Hence, one approach to designing a magnetization distribution of a required shape is to approximate the shape by superimposing a set of

known distributions. Many distributions of practical interest may be described by a cosine series and discussion in the following sections is, for clarity, limited to the cosine rather than the full series. Results for the full series may be readily derived, if required.

Fig. 2(a) to (f) shows the relative fall off in applied field $H(x)$ and in axial magnetization component $M(x)$ for a range of drive strap geometries. The plots are for a 1 μm thick cylindrical permalloy film of 5.0 mil diameter. Curves a, b, c, d correspond to drive strap half widths of 1.0, 5.0, 10.0, 20.0 mils, respectively. In Fig. 2(a), (b) the distance between drive strap (or return strap) and film axis is 3.5 mils. Fig. 2(c), (d) and (e), (f) correspond, respectively, to a distance of 5.0 and 10.0 mils. It can be noted that the magnetization distributions extend to a considerable distance and do not vary as strongly as the applied field. The fields of Fig. 2(a), (c), (e) are shown to normalized scale, however, the peak field or drive current required to just saturate the axial component at $x = 0$ varies significantly with geometry, and is shown in Fig. 3.

In a plated wire memory, the local state of a region of film may be assigned as positive or negative depending on the remanent circumferential component of magnetization. To read out the circumferential component in a nondestructive manner, a local axial field is applied by a drive strap surrounding the wire at the location of interest, and the signal appearing across the ends of the plated wire is measured. The signal is due to the circumferential flux change integrated along the wire (neglecting capacitive or other emfs). The circumferential component distribution is obtained simply from the axial component using the relation, $M(\text{circumferential}) = (M^2 - M(\text{axial})^2)^{\frac{1}{2}}$. The total area under this curve is proportional to the signal obtained when the circumferential component has been set completely into one direction. It is convenient to equate the integrated circumferential component to an equivalent length of film that has everywhere a 90° rotation of magnetization. Fig. 4 shows the equivalent lengths of film for the curves of Fig. 2.

If now a locally reversed region is established and the readout field applied again, the signal will have decreased, since the reversed region contributes to the signal with reversed sign. It has been found previously[6] that the presence of a domain wall has little effect on the macroscopic magnetization distribution; hence, the curves of Fig. 2 may be used to estimate the new signal. In this case, the area under the circumferential plot is taken negatively over the length of the reversed

region and positively for the remainder. Fig. 5 shows curves of net equivalent length versus width of reversed region. Curves a, and b correspond to strap half width of 1.0 mil but half separations of 3.5 and 5.0 mils, respectively. Curves c and d correspond to strap half width of 10.0 mils, and half separations of 5.0 and 10.0 mils, respectively.

IV. NONUNIFORM FIELDS LARGE ENOUGH TO PRODUCE LOCAL SATURATION

When the local effective field reaches the value H_K then the local magnetization rotation has the value $\pi/2$; hence, $M(x) = M$, the

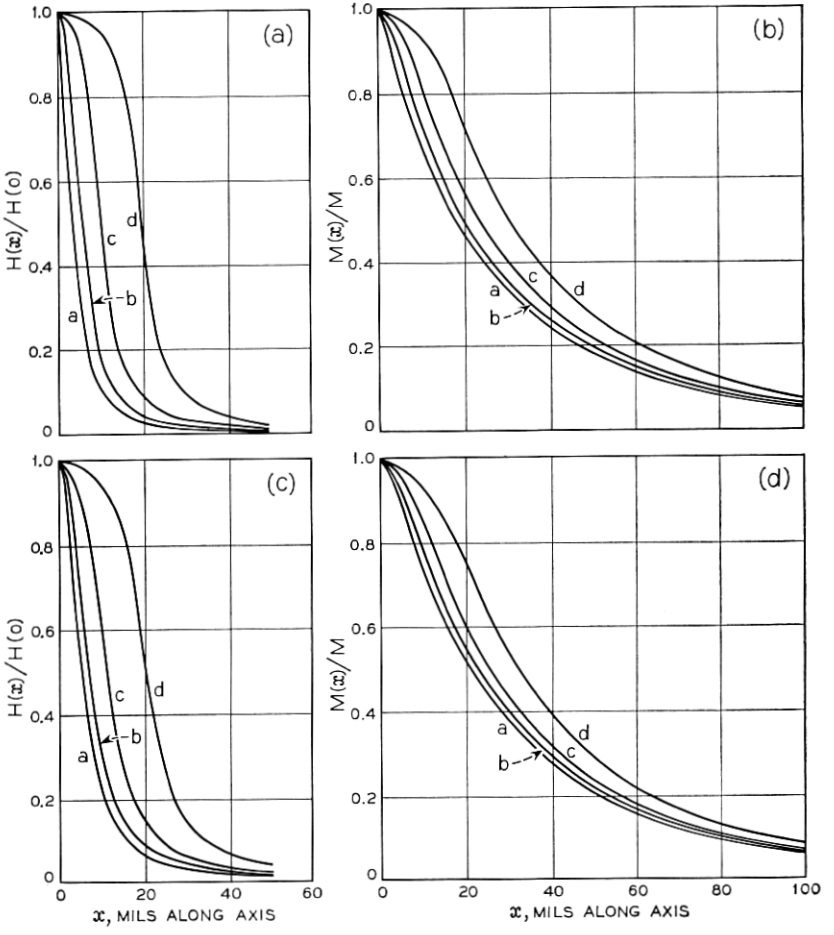

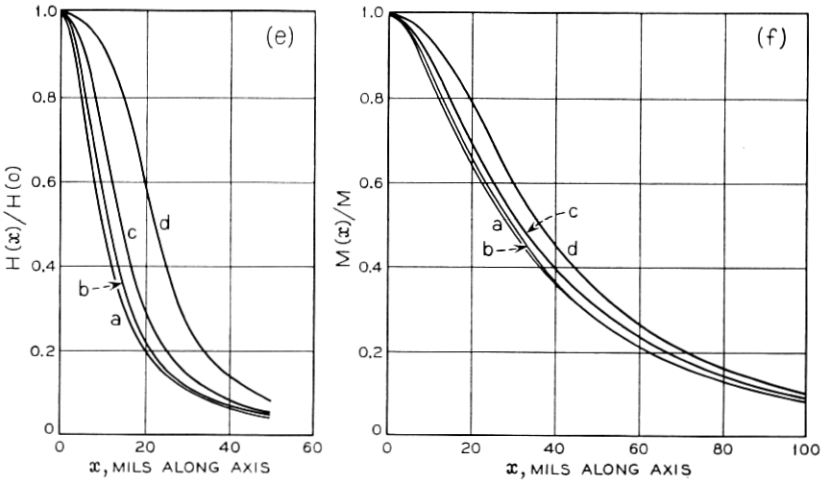

Fig. 2 — The curves denoted a, b, c, d refer, respectively, to a parallel drive strap arrangement of half widths 1.0, 5.0, 10.0, and 20.0 mils. (a) and (b) correspond to a strap-to-film axis distance of 3.5 mils, (c) and (d) correspond to 5.0 mils and (e) and (f) to 10.0 mils. (a), (c), and (e) give to normalized scale the field $H(x)/H(0)$ applied along the axis of a 5.0 mil diameter, 1μm thick cylindrical permalloy film with $H_K = 3.0$. (b), (d), and (f) show the resulting axial magnetization components $M(x)/M$ due to the actual (i.e., non-normalized) applied field.

saturation value. A further increase in the field cannot therefore, produce any further increase in $M(x)$ and it is necessary to modify the preceding discussion to take the effect of saturation into account.

We assume that the magnetization distribution is monotonic, and the width of the saturated region is specified at the outset. The current required to produce this degree of saturation may then be found for a given drive strap geometry, and the resulting magnetization distribution is calculated. This somewhat arbitrary procedure renders the problem tractable.

If the film has saturated over a region $-R \leqq x \leqq R$ then the material within this region has $M(x) = M$ a constant; hence, $dM(x)/dx$ vanishes within this region. It is convenient to introduce a modifying function $S(x)$, having period λ, that is zero over the range $-R \leqq x \leqq R$, but is otherwise unity. The product $S(x)dM(x)/dx$ then has the property of being zero over $-R \leqq x \leqq R$ but is otherwise equal to $dM(x)/dx$. By introducing this product into the integral for the demagnetizing field in place of $dM(x)/dx$, we have effectively modified the integral without changing the limits of integration. Let

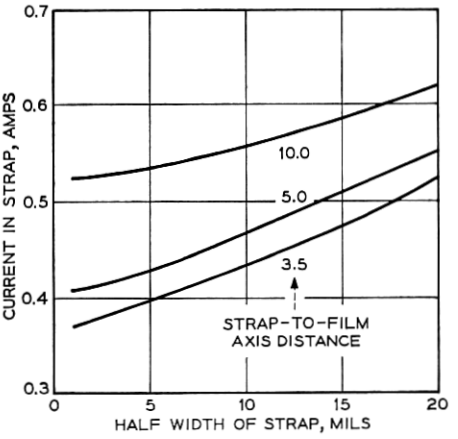

Fig. 3 — Current in drive strap required to just saturate the film of Fig. 2 at $x = 0$, for the several drive strap geometries of Fig. 2.

$H(x)$ and $M(x)$ be represented by the finite series

$$H(x) = \sum_{0}^{N} h_n \cos 2\pi nx/\lambda, \qquad M(x) = M \sum_{0}^{N} m_n \cos 2\pi nx/\lambda,$$

also let $S(x)$ be represented by a cosine series, then

$$S(x) = \sum_{n=0}^{\infty} s_n \cos 2\pi nx/\lambda,$$

where for the required step function

$$s_0 = 1 - (2R/\lambda), \qquad s_n = -\frac{4R}{\lambda}\left(\frac{\sin 2\pi nR/\lambda}{2\pi nR/\lambda}\right), \qquad n > 0.$$

Differentiating the series for $M(x)$, we have

$$\frac{dM(x)}{dx} = -\frac{2\pi M}{\lambda} \sum_{n=0}^{N} n m_n \sin 2\pi nx/\lambda.$$

Then the product may be written,

$$S(x)\frac{dM(x)}{dx} = -\frac{2\pi M}{\lambda} \sum_{j=0}^{\infty} \sum_{n=0}^{\infty} s_j n m_n \cos 2\pi jx/\lambda \sin 2\pi nx/\lambda$$

$$= -\frac{\pi M}{\lambda} \sum_{j=0}^{\infty} \sum_{n=0}^{N} s_j n m_n (\sin 2\pi(j+n)x/\lambda - \sin 2\pi(j-n)x/\lambda).$$

This represents a series of the form $A_0 + A_1 \sin 2\pi x/\lambda + \ldots$ and we may rearrange by grouping the coefficients to obtain

$$S(x)\frac{dM(x)}{dx} = -\frac{\pi M}{\lambda}\sum_{p=1}^{N} p s_p m_p - \frac{\pi M}{\lambda}\sum_{n=1}^{N}\left[\sum_{p=1}^{N}(s_{|p-n|} - s_{p+n} + s_0\delta_p^n)pm_p\right]\sin 2\pi nx/\lambda,$$

where $\delta_p^n = 1$ when $p = n$, but is otherwise zero, and the series for $S(x)$ is terminated for subscripts greater than $2N$. Using this final series in place of the series for $dM(x)/dx$ in the integral (3) for the demagnetizing field we obtain,

$$H_m(x) = \sum_{n=1}^{N}\left\{\frac{1}{2n}\sum_{p=1}^{N}(s_{|n-p|} - s_{n+p} + s_0\delta_p^n)pm_p\right\}\alpha_n \cos 2\pi nx/\lambda, \qquad (9)$$

where the α_n have the values calculated previously for the nonsaturating case. There are now several conditions that the magnetization distribution must satisfy: it has the value $M(x) = M$ over the range $-R \leqq x \leqq R$ and satisfies the torque equation (6) outside this range, and finally, the amplitude of the applied field is such that $M(x)$ determined from (6) has also the value M at $x = \pm R$. The required field value is given by the calculation for any particular drive strap

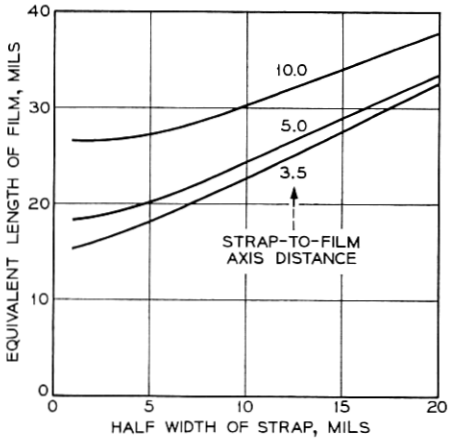

Fig. 4 — The change in circumferential component of magnetization averaged along the film is proportional to the signal obtained during readout. This is expressed in terms of equivalent length of film that would produce the same signal when uniformly excited to saturation. The plots are derived from the axial component distributions of Fig. 2.

configuration. We now substitute the series (1), (2), and (9) into the torque equation (6) and gathering coefficients, we obtain,

$$H_K m_0 = h_0 \quad \text{for} \quad n = 0$$

and the set of N equations,

$$H_K m_n + \sum_{p=1}^{N} \frac{p\alpha_n}{2n} (s_{|n-p|} - s_{n+p}) m_p + \frac{s_0}{2} \alpha_n m_n = h_n ,$$
$$n = 1, 2, \cdots , N. \qquad (10)$$

These N equations constitute a set of linear simultaneous equations in the N unknown coefficients m_n. These equations may be expressed,

$$\sum_{p=1} c_{np} m_p = h_n , \qquad n = 1, 2, \cdots , N,$$

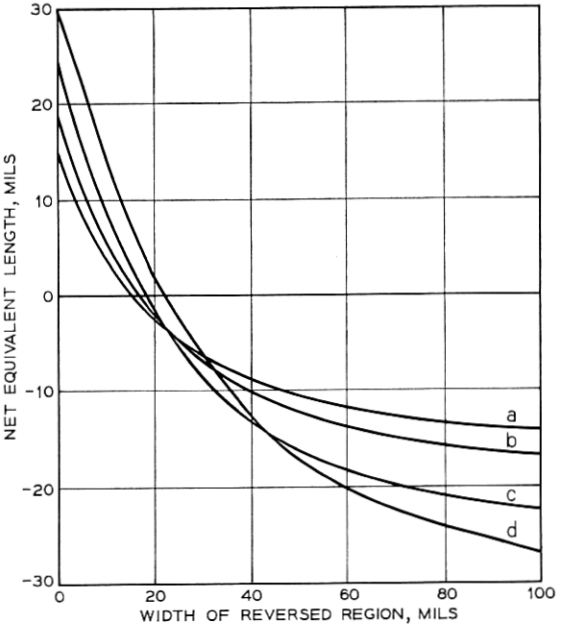

Fig. 5 — Change in net equivalent length of film (proportional to output signal during NDRO), versus width of reversed domain established beneath drive strap. Curves a, b refer to strap half width of 1.0 mils, and strap to film axis distances of 3.5 and 5.0 mils, respectively. Curves c and d refer to strap half width of 10.0 mils and strap to film axis distances of 5.0 and 10.0 mils, respectively. The curves are derived from the axial distributions of Fig. 2.

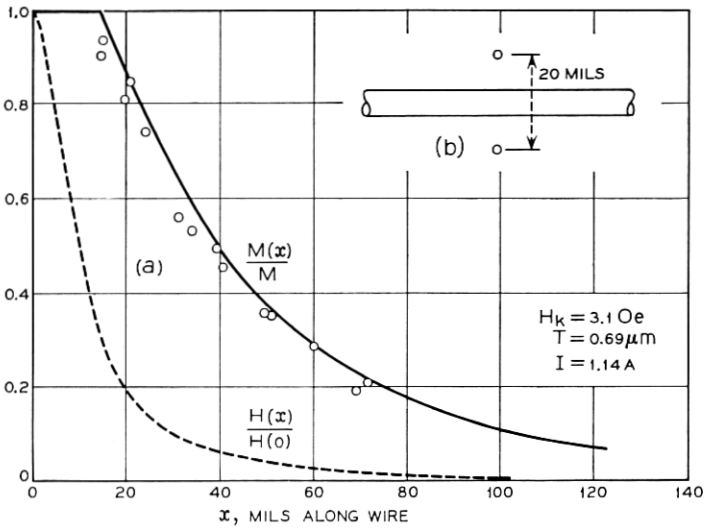

Fig. 6 — (a) Theoretical curve and experimental points taken with the Kerr effect probe[9] for a saturated cylindrical film. The broken curve shows the relative fall off of the axial applied field. (b) The field is applied by a parallel drive wire arrangement shown in cross section. The current I applied in the drive wires is 1.14 A.

where the c_{np} are given by

$$c_{np} = \left\{\frac{p\alpha_n}{2n}\left(s_{|n-p|} - s_{n+p}\right) + \left(\frac{s_0}{2}\alpha_n + H_K\right)\delta_n^p\right\}.$$

Such a set of equations may be conveniently inverted by computer for any particular case giving the m_n coefficients in terms of the h_n's. Since the m_n and h_n coefficients are linearly related, a scale factor, e.g., current in drive strap, is applied to $H(x)$ to ensure that the distribution has a value M at $x = \pm R$. The resulting series indicates a non-uniform distribution for $M(x)$ within the range $-R \leqq x \leqq R$, but, by the action of $S(x)$, this produces no demagnetizing field and therefore does not influence the distribution obtained outside the range. The value of $M(x)$ is therefore set equal to M inside the saturation range. The plot obtained within this range reflects instead the value of $(H - H_m)/H_K$.

Fig. 6(a) shows a plot of the axial magnetization distribution where the film has saturated over a length of 30 mils, for a cylindrical film of 5.2 mil diameter, 0.69μm thickness and $H_K = 3.1$ Oe. The broken

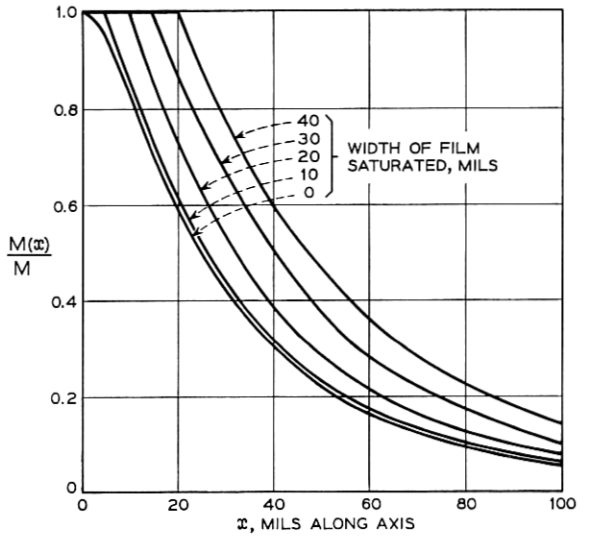

Fig. 7 — Axial component of magnetization for the cylindrical film of Fig. 6 when driven to different degrees of saturation.

curve of Fig. 6(a) shows a normalized plot of the applied field. The field is applied by a drive wire, and the separation between drive and return wire is 20 mils as shown in 6(b). The calculation indicates a current of 1.14 amps to produce this degree of saturation. The points represent measurements made previously[6] using the Kerr Effect probe.

Fig. 7 shows the axial magnetization component for the geometry of Fig. 6 where the film has saturated to widths of 0, 10, 20, 30, 40 mils. The applied field is shown in Fig. 8, curve a, versus width of saturated region produced by the field. Curve b is for a drive strap of half width 10 mils and strap to film axis distance of 10 mils. The shape of the curve does not appear to vary markedly with drive strap geometry. It can be noted that little increase in current is required to extend the saturated region from 1 to 10 mils, but that saturation to greater widths requires increasingly larger currents.

V. FILM THICKNESS VARIATION

Now let $T(x)$ be the variable film thickness and assume that $T(x)$ and $H(x)$ have the same periodic distance λ, then we may write

$$T(x) = \sum_{n=0}^{\infty} t_n \cos(2\pi n x/\lambda).$$

In the thin film approximation, magnetization variations within the thickness of the film are neglected and demagnetizing fields are calculated from the net pole density per unit area of film. To take into account a variation in thickness we take the product $T(x)M(x)$ as the total magnetization component in the hard direction and evidently the pole density is then given by $-(d/dx)\,[T(x)M(x)]$.

Taking the product of the series, we obtain

$$T(x)M(x) = \frac{M}{2}\left\{t_0 m_0 + \sum_{p=0}^{N} t_p m_p + \sum_{n=1}^{N}\sum_{p=0}^{N} m_p[(t_{n+p} + t_{|n-p|}) + t_0\delta_n^p]\cos 2\pi nx/\lambda\right\},$$

hence, replacing $M(x)$ by $T(x)M(x)$ in (3), the demagnetizing field is given by

$$H_m(x) = \sum_{n=0}^{N}\frac{\alpha_n}{2}\sum_{p=0}^{N} m_p(t_{n+p} + t_{|n-p|} + t_0\delta_n^p)\cos 2\pi nx/\lambda, \qquad (11)$$

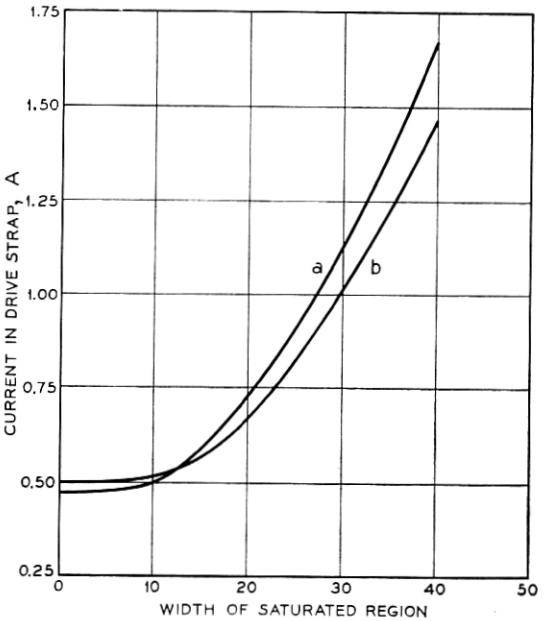

Fig. 8—Current required to produce a given width of saturated region along a cylindrical film of radius 2.6 mils, thickness 0.69μm, H_K = 3.1 Oe. Curve a is for the arrangement of Fig. 6. Curve b is for a parallel conductor drive strap of width 20 mils situated at $\pm$10 mils from the film axis.

where $\delta_n^p = 1$ when $n = p$ but is otherwise zero. Substituting into the torque equation (6), and equating coefficients we have finally

$$H_K m_0 = h_0$$

and

$$\sum_{p=0}^{N} \left[\frac{\alpha_n}{2} (t_{n+p} + t_{|n-p|} + t_0 \delta_n^p) + H_K \delta_n^p \right] m_p = h_n , \qquad n = 1, 2, \cdots, N$$

i.e.,

$$\sum_{p=1}^{N} \left[\frac{\alpha_n}{2} (t_{n+p} + t_{|n-p|} + t_0 \delta_n^p) + H_K \delta_n^p \right] m_p = h_n - \alpha_n t_n h_0 / H_K . \qquad (12)$$

This last expression represents a set of linear simultaneous equations which may be solved numerically to give the coefficients m_n in terms of t_n and h_n. The calculation, when applied to the case of a flat film strip having an ellipsoidal cross section along the hard direction, subject to a uniform field, predicts a uniform demagnetizing field of magnitude very close to that indicated by the tables of Osborne[9] based on the solution of Maxwell's equation for the general ellipsoid. Fig. 9 shows the magnetization distribution near an edge of a uniform thickness (0.22 μm) flat film with $H_K = 2.62$ Oe. The points represent data taken with the Kerr effect probe.

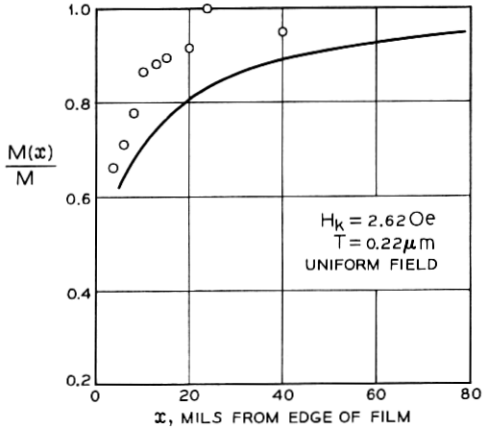

Fig. 9 — Magnetization component near the edge of a flat film of thickness 0.22μm, and $H_K = 2.62$ Oe. The applied field is uniform and equal to H_K. The edge runs parallel to the film easy direction. The points show measurements taken with the Kerr effect probe.

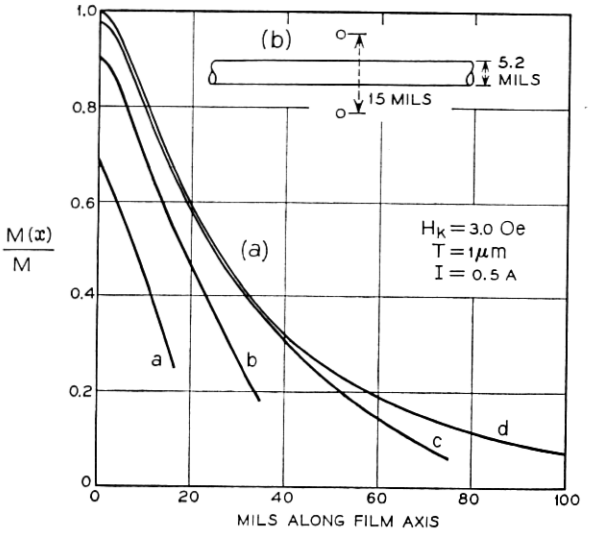

Fig. 10 — Axial magnetization component for cylindrical film segments of differing length due to the field from a parallel wire drive strap at distance ±7.5 mils from film axis. Curves a, b, and c refer to segments of length 40, 80, 160 mils, respectively. d refers to a continuous film. The current in the drive wire is 0.5 A. (b) shows a cross section of the drive wire arrangement.

Fig. 10 shows, for comparison the magnetization distribution for a nonsaturating hard direction field applied to 5.2 mil diameter cylindrical film segments of differing lengths, but uniform thickness of 0.7μm, and $H_K = 3.0$. The field is applied by a parallel drive wire arrangement of separation 15 mils. Finally, Fig. 11 shows the axial magnetization distribution for a uniform field applied to a cylindrical film having a circumferential cut. Film radius is 2.6 mils, thickness is 1.0 μm and $H_K = 3.0$ Oe. It is to be noted that the present technique has a spatial resolution limited both by the number of terms of the series that can be retained for computation, and by the basic limitation that exchange forces are neglected. We cannot, therefore, expect to obtain detail of magnetic behavior very close to an edge, for example, or for an extremely narrow scratch.

VI. ANISOTROPY MAGNITUDE VARIATION

Let us assume that the anisotropy constant is represented by a cosine series, i.e.,

$$K(x) = \sum k_n \cos 2\pi nx/\lambda.$$

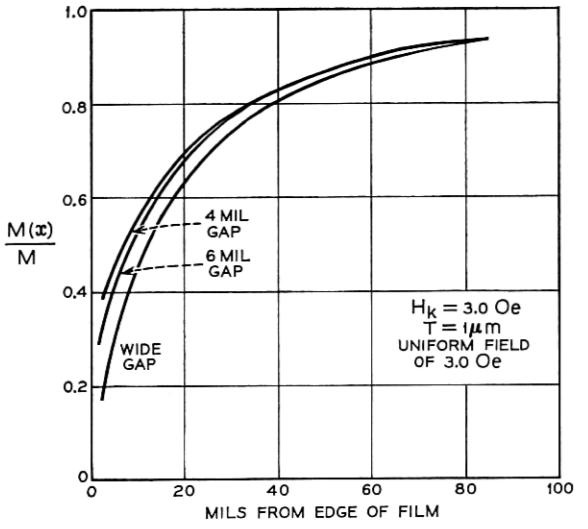

Fig. 11 — Plot of axial magnetization component for a 5.2 mil diameter cylindrical film with a circumferential gap. The curves show the result for a 4 mil, 6 mil and wide gap. The axial applied field is uniform and equal to 3.0 oe. Film thickness is 1.0μm and $H_K = 3.0$ Oe.

Then substituting into the torque equation (6), and gathering terms we find

$$\sum_{p=0}^{N} \frac{1}{M} (k_p + k_0 \delta_p^0) m_p = h_0 \tag{13}$$

and

$$\sum_{p=0}^{N} \left\{ \frac{1}{M} (k_{n+p} + k_{|n-p|} + k_0 \delta_p^n) + \alpha_p \delta_p^n \right\} m_p = h_n \,,$$

$$n = 1, 2, \cdots, N. \tag{14}$$

Together these equations represent $N + 1$ linear simultaneous equations in $N + 1$ unknown coefficients m_p, and may be solved by computer. This calculation may be used for example to find the local behavior of **M** at the junction between two regions with differing anisotropy constants, or to find the effective permeability of a film having some systematic variation in anisotropy constant. A simplified discussion of this latter problem has been given previously.[10] Fig. 12 shows the effect of using a high H_K buffer region surrounding a normal H_K section of film. Curve a shows the distribution for a uniform wire with $H_K = 3.0$, b shows the

modification when H_K is increased to a value $H_K = 15$ for all distances beyond $x = 10$ mils and c shows the result when H_K is further increased to 30 oe in the buffer region. The effectiveness of the high H_K buffer region in sharpening the distribution can be noted. This is achieved, however, at the expense of greater current required to just saturate at $x = 0$. For curves a, b, c the currents are 0.50, 0.79, and 0.93 A, respectively. Fig. 12(b) shows a cross section of the parallel conductor drive strap arrangement.

VII. FIELD EXTERNAL TO FILM

Combs and Wujek[11] have calculated the field external to a thin film rectangular slab assuming a pole distribution concentrated at the edges of the slab. We now calculate the field external to a continuous film subject to various applied field conditions where the details of the effective pole distribution form the essential part of the problem. The results of previous sections may be adapted to find the field external to films which have a hard axis variation in thickness or anisotropy

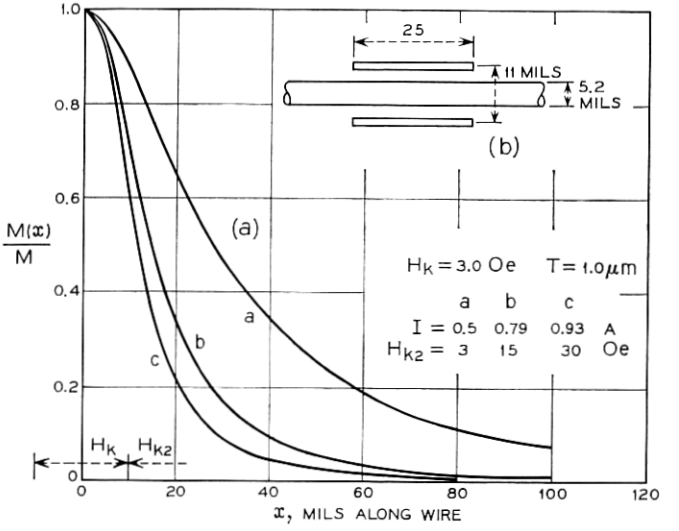

Fig. 12 — (a) Effect of high H_K buffer region surrounding a normal H_K section of cylindrical film. Curve a shows the magnetization component for a uniform film with $H_K = 3.0$. Curves b and c show the result when H_K is increased to 15 and 30 Oe, respectively for distances greater than 10 mils to either side of the drive strap centerline. (b) Details of drive strap arrangement. The currents required to just saturate the film at $x = 0$ are 0.5, 0.79, and 0.93 A for the cases a, b, and c, respectively.

but these cases are not considered in detail here. Consider the field at some distance d from the surface of a flat film and at distance x along the hard axis. The external field H_m parallel to the film due to the distribution of poles over the film surface may be found by evaluating the integral

$$H_{me}(x, d) = \int_{-\infty}^{\infty}\int_{-\infty}^{\infty} -\frac{\frac{dM(x)}{dx}(x - X)\,dX\,dY\,T}{[d^2 + Y^2 + (X - x)^2]^{\frac{3}{2}}}. \tag{15}$$

Substituting for $M(x)$ and performing the integration we find

$$H_{me}(x, d) = -\frac{4\pi^2 MT}{\lambda}\sum_{n=1}^{\infty} n m_n e^{-2\pi dn/\lambda}\cos 2\pi nx/\lambda. \tag{16a}$$

This is the external field parallel to the plane of the film given as a function of distance d from the film. For a cylindrical film the result is

$$H_{me}(x, d) = -4\pi aTM\sum_{n=1}^{\infty}\left(\frac{2\pi n}{\lambda}\right)^2 K_0(2\pi nd/\lambda) \cdot I_0(2\pi na/\lambda)m_n\cos 2\pi nx/\lambda, \tag{16b}$$

where a is the cylinder radius, and d is the distance from cylinder axis to the location at which the axial component of field is measured, $(d > a)$. The field inside the cylinder may be similarly derived, the result is

$$H_{me}(x, d) = -4\pi aTM\sum_{n=1}^{\infty}\left(\frac{2\pi n}{\lambda}\right)^2 K_0(2\pi na/\lambda)I_0(2\pi nd/\lambda)m_n\cos 2\pi nx/\lambda,$$

where now $d < a$. Along the cylinder axis $I_0(0) = 1$. Fig. 13 shows a plot of the axial component of the demagnetizing field for several values of distance from film axis. The cylindrical film is assumed to have a diameter of 5.2 mils, $H_K = 3.0$ Oe, thickness is 1.0μm, and is excited by a one turn loop of radius 7.5 mils.

The flux coupling a parallel wire loop parallel to a flat film surface and to the film easy direction with the conductors at $\pm D$ from the surface may now be found. The flux F per unit length of the parallel conductor loop is then

$$F = 4\pi M(x)T - 2\int_0^D H_{me}(x, z)\,dz.$$

Substituting for H_{me} and rearranging, we find

$$F = 4\pi MT\sum_{n=0}^{N} m_n e^{-2\pi nD/\lambda}\cos 2\pi nx/\lambda. \tag{17}$$

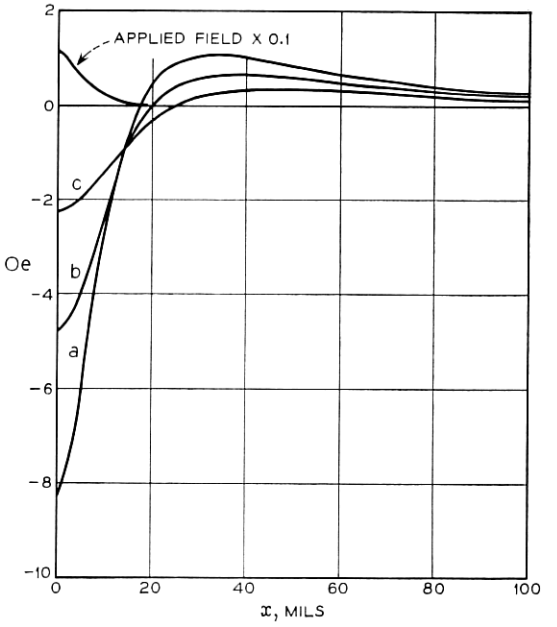

Fig. 13 — External axial component of field due to the distribution of magnetization along a cylindrical film. (The field due to the drive strap is not included.) The field is plotted along lines parallel to the film axis, at several distances from the axis. The film has a thickness of 1μm, $H_K = 3.0$ Oe, diameter 5.2 mils, and is subject to the field from a one turn circular loop of diameter 15 mils. Curves a, b, and c refer to distances of 2.6, 5.0, and 10 mils from the axis, respectively.

If the magnetization distribution is due to the field from a parallel wire loop with conductors at $\pm d$ from the film surface, then using expression (8a), we have

$$\frac{F(x)}{4\pi T} = \frac{\pi CIM}{\lambda H_K} + \frac{2\pi CIM}{\lambda} \sum \frac{e^{-2\pi n(D+d)} \cos 2\pi nx/\lambda}{H_K + \alpha_n}. \qquad (18a)$$

It can be noted that $F(x)/4\pi T$ is formally equivalent to the magnetization component in the film at the plane of the loop due to a current I in a loop with conductors at $\pm(D + d)$ from the film. The mutual inductance between two loops (not necessarily enclosing the film) may then be found directly from the above results.

The flux linkage between the film and drive loop is obtained by setting $x = 0$ and $D = d$. A current I in the loop gives rise to a magnetization component $M(0, I, d)$ at $x = 0$, and the flux linking the loop is

given by $M(0, I, 2d)$, using (18a). The fractional flux linkage is therefore $M(0, I, 2d)/M(0, I, d)$.

At $x = 0$, the expression (18a) may be evaluated in closed form; the result is,

$$\frac{F(0)}{4\pi T} = -\frac{2IC}{4\pi MT} \exp(2dH_K/4\pi MT)E_i(-2dH_K/4\pi MT).$$

Hence the fractional flux linkage (FFL) is

$$\text{FFL} = \exp(\mu d)E_i(-2\mu d)/E_i(-\mu d),$$

where $\mu = 2H_K/4\pi MT$ and E_i is the exponential integral. This is a useful parameter which shows the degree of coupling between loop and film, and is plotted in Fig. 14 as a function of d, for a flat film of thickness 0.1μm, $H_K = 4.0$ Oe.

The result for cylindrical films is more complicated. In this case it can be shown that

$$\frac{F(x)}{4\pi T} = \frac{2CI\pi M}{\lambda} \cdot \sum_{1}^{\infty} \frac{d\left(\frac{2\pi n}{\lambda}\right)^3 K_0\left(\frac{2\pi nD}{\lambda}\right) I_0\left(\frac{2\pi na}{\lambda}\right) K_1\left(\frac{2\pi nd}{\lambda}\right) I_0\left(\frac{2\pi na}{\lambda}\right) \cos\frac{2\pi nx}{\lambda}}{H_K + \frac{4\pi MT}{a}\left(\frac{2\pi na}{\lambda}\right)^2 K_0\left(\frac{2\pi na}{\lambda}\right) I_0\left(\frac{2\pi na}{\lambda}\right)}, \quad (18b)$$

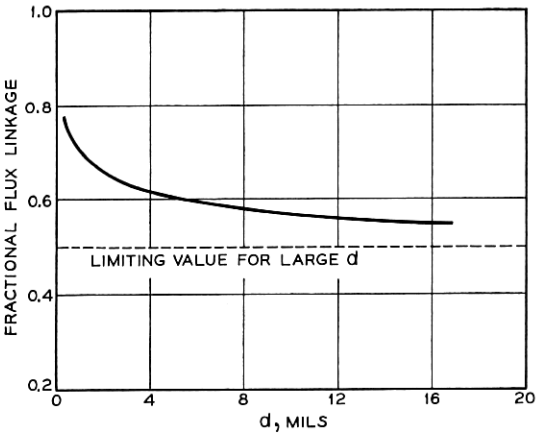

Fig. 14 — Fractional flux linkage between a flat film of thickness 0.1μm, H_K = 4.0 Oe, and a pair of parallel wire conductors as a function of distance from film to the conductors. The parallel wire conductors serve as both drive and sense windings.

where the cylinder has radius a, thickness T and is excited by the field from a circular loop of radius d. $F(x)$ gives the amount of flux picked up by a loop of radius D at an axial distance x from the drive loop.

VIII. INTERACTION BETWEEN PARALLEL FILMS

Consider two plane parallel films (denoted 1 and 2) of thickness T and T' and anisotropy fields H_K and H_K', respectively, separated by a distance w along a normal to the film's surface. A nonuniform field is applied along the (parallel) hard directions by a drive strap. Let the hard direction fields be $H(x)$ and $H'(x)$. The field acting on film 1 due to the distribution within film 2 we denote by $H(x)_{12}$, and similarly the field acting on 2 due to film 1 is $H(x)_{21}$. These fields are taken to act along the film's common hard direction, and the films are assumed to be sufficiently thin that fields normal to the surface have negligible effect.

The torque equation determining the local rotation of magnetization within the two films may be written

$$H_K \sin \theta(x) = H(x) + H_m(x) + H_{12}(x), \quad \text{film 1} \tag{19}$$

$$H_K' \sin \theta'(x) = H'(x) + H_m'(x) + H_{21}(x), \quad \text{film 2.} \tag{20}$$

Let $M(x)$, $M'(x)$ be the hard direction components of magnetization in the two films, then from previous sections we have (assuming cosine distributions)

$$H(x) = \sum h_n \cos 2\pi nx/\lambda$$

$$H'(x) = \sum h_n' \cos 2\pi nx/\lambda$$

$$H_m(x) = -\beta T \sum n m_n \cos 2\pi nx/\lambda, \quad H_m'(x) = -\beta T' \sum n m_n' \cos 2\pi nx/\lambda$$

$$H_{12}(x) = -\beta T' \sum n m_n' \exp(-2\pi nw/\lambda) \cos 2\pi nx/\lambda$$

$$H_{21}(x) = -\beta T \sum n m_n \exp(-2\pi nw/\lambda) \cos 2\pi nx/\lambda,$$

where $\beta = 4\pi^2 M/\lambda$. Noting that $\sin \theta(x) = M(x)/M$ and $\sin \theta'(x) = M'(x)/M$, we substitute the above series into the two torque equations and equating coefficients, we obtain,

$$\left.\begin{aligned} H_K m_n &= h_n - \beta n T m_n - \beta n T' m_n' \exp(-2\pi nw/\lambda) \\ H_K' m_n' &= h_n' - \beta n T' m_n' - \beta n T m_n \exp(-2\pi nw/\lambda) \end{aligned}\right\}.$$

Solving for m_n and m_n', we have finally

$$m_n = \left[h_n - \frac{\beta n T' h_n' \exp(-2\pi nw/\lambda)}{H_K' + \beta n T'}\right] \cdot \left[H_K + \beta n T - \frac{\beta^2 n^2 T T' \exp(-4\pi nw/\lambda)}{H_k' + \beta n T'}\right]^{-1} \tag{21}$$

$$m_n' = \left[h_n' - \frac{\beta n T h_n \exp(-2\pi n w/\lambda)}{H_K + \beta n T}\right] \cdot \left[H_K' + \beta n T' - \frac{\beta^2 n^2 T T' \exp(-4\pi n w/\lambda)}{H_K + \beta n T}\right]^{-1}. \quad (22)$$

These expressions can be compared with the results when the films are present singly, i.e., at large separations,

$$m_n = (h_n)(H_K + \beta n T)^{-1}$$
$$m_n' = (h_n')(H_K' + \beta n T')^{-1}.$$

Evidently the calculation can be extended to a greater number of layers and it is immaterial whether the drive fields are applied positively or negatively provided the fields are appropriately assigned, that is, the field may be generated by conductors located between or completely to one side of the films. The equations relating the coefficients m_n, m_n' may be concisely expressed in matrix form,

$$\left\{\begin{bmatrix} H_K & 0 \\ 0 & H_K' \end{bmatrix} - \beta n \begin{bmatrix} T & 0 \\ 0 & T' \end{bmatrix} - \beta n \exp(-2\pi n w/\lambda) \begin{bmatrix} 0 & T \\ T' & 0 \end{bmatrix}\right\} \begin{bmatrix} m_n \\ m_n' \end{bmatrix} = \begin{bmatrix} h_n \\ h_n' \end{bmatrix}. \quad (23)$$

The three matrix terms of the left-hand side represent in turn the effect of anisotropy, demagnetizing field, and interaction between films. The extension to three or more films is straightforward. Fig. 15 shows the effect of flux closure between two films only 2 mils apart subjected to the field from a drive wire sandwiched between them. The films have equal thickness of 0.1 μm and anisotropy field $H_K = 4.0$ Oe. Since the fields are applied in opposite directions in the two films the demagnetizing fields tend to cancel and the magnetization distribution widths are smaller than for similar films well spread apart. Curve a shows the coupled distribution, and b shows the distribution with one film removed. The current required to just saturate the films is 0.127 A, with one film removed the current required rises to 0.170 A. With films of thickness 1000 Å, separations of order a few mils are essential for this effect to be appreciable.

We may use the results (21) and (22) to examine the effect of a keeper layer. The action of the keeper is to modify the field applied to the film and to provide some degree of flux closure. Consider the case of a flat film situated between two drive wires, distance d from the film, with a keeper layer distance $w > d$ from the film. Let primed quantities refer to the keeper, and unprimed refer to the film. The keeper typically has a

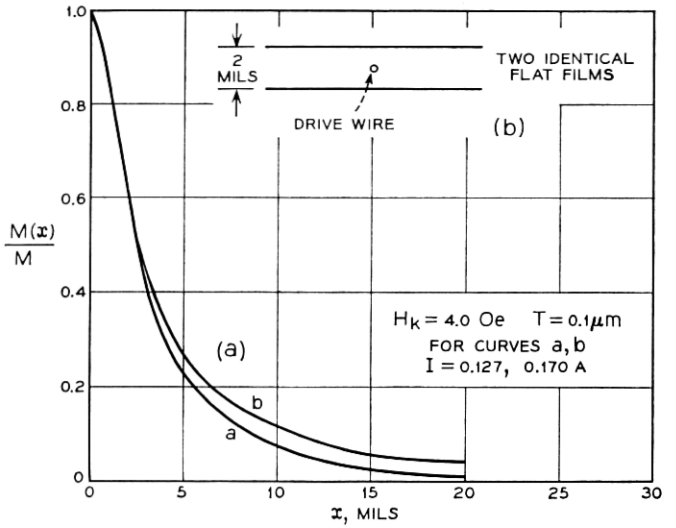

Fig. 15 — (a) Effect of flux closure between two identical flat films, separated by a distance of 2 mils. The field is applied by a single wire placed between the films as shown in (b). The films have a thickness of 0.1μm and $H_K = 4.0$ Oe. Curve b shows the result when one of the films is removed. The current required to just saturate the films at $x = 0$ now rises from the bifilm value 0.127 A to 0.170 A for a single film.

thickness of mils or tens of mils and hence $4\pi^2 MT'/\lambda \gg H_K'$ for reasonable values of M and λ. Equation (21) then reduces to,

$$m_n = [h_n - h_n' \exp(-2\pi nw/\lambda)]/[H_K + \beta nT(1 - \exp(-4\pi nw/\lambda)]. \quad (24)$$

The field applied to the film in the absence of the keeper is $H(x) = \sum h_n \cdot \cos 2\pi nx/\lambda$, where for the present case

$$h_0 = \frac{2CI\pi}{\lambda}, \qquad h_n = \frac{4CI\pi}{\lambda} \exp(-2\pi nd/\lambda).$$

I is the current in the drive wires. The field applied to the keeper is given by $\sum h_n' \cos 2\pi nx/\lambda$ where $h_0' = 0$,

$$h_n' = \frac{2CI\pi}{\lambda} \{\exp(-2\pi n(w + d)/\lambda) - \exp(-2\pi n(w - d)/\lambda)\}.$$

Then, $m_0 = 2CI\pi/\lambda H_K$, and

$$m_n = CI(2\pi/\lambda)[2 \exp(-2\pi nd/\lambda) - \exp(-2\pi n(2w + d)/\lambda) + \exp(-2\pi n(2w - d)/\lambda)]/[H_K + \beta nT(1 - \exp(-4\pi nw/\lambda))]. \quad (25)$$

It can be noted that the terms in the numerator are equivalent to the coefficients of the field due to the drive strap directly, and to images of the drive straps, with the keeper as mirror. The image property of the keeper layer is well known and has had considerable application to the discussion of keepers, see, for example, Refs. 12 and 13. The effect of the mutual interaction between keeper and film is to modify the α_n factors ($\alpha_n = \beta nT$ for a flat film) by a term $1 - \exp(-4\pi nw/\lambda)$. The influence of this term is two fold, (*i*) the spreading of the magnetization component is reduced and (*ii*) the drive field required is reduced.

Fig. 16 shows the effect of a keeper layer on the distribution in a flat film of thickness 0.2μm, $H_K = 4.0$ Oe. Field is supplied by a pair of drive straps of width 10 mils carrying a current of 0.22 A, at a distance of 5 mils from the film. The keeper layer is taken to be 6 mils from the film. Curve a shows the hard direction component in the absence of the keeper, b shows the effect only of the image fields due to the presence of the keeper, and c shows the final result when image fields and partial flux closure are taken into account.

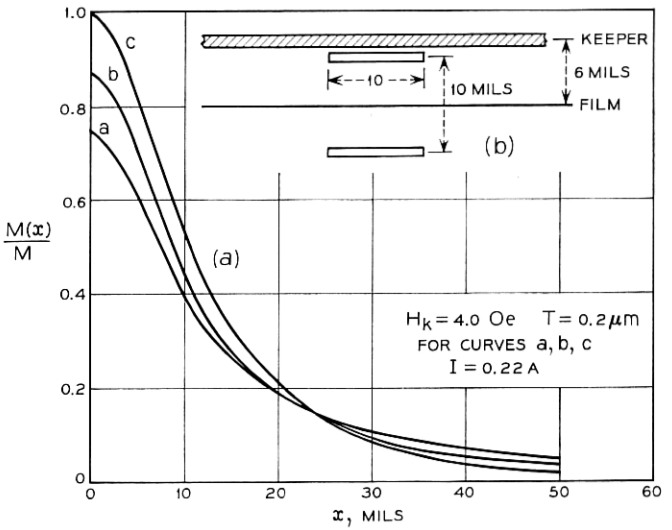

Fig. 16—(a) Effect of a keeper layer on the magnetization distribution in a flat film of thickness 0.2μm, $H_K = 4.0$ Oe. Field is applied by parallel drive straps of width 10 mils at ± 5 mils from the film. The keeper layer is taken to be 6 mils from the film as shown in (b). Curve a shows the hard direction component in the absence of the keeper, Curve b shows the effect of the image fields only when the keeper is present, and Curve c shows the final result when image fields and flux closure are taken into account.

The effects of a flat keeper layer on the response of a cylindrical film are not amenable to calculation by the present method owing to the mixed geometry.

The case of a cylindrical film with a concentric cylindrical keeper is next considered. The discussion closely parallels that for flat films and leads to a result analogous to (24),

$$m_n = \left[h_n - h_n' \frac{I_0\left(\frac{2\pi na}{\lambda}\right)}{I_0\left(\frac{2\pi nA}{\lambda}\right)} \right] \cdot \left[H_K + \alpha_n \left[1 - \frac{I_0\left(\frac{2\pi na}{\lambda}\right) K_0\left(\frac{2\pi nA}{\lambda}\right)}{I_0\left(\frac{2\pi nA}{\lambda}\right) K_0\left(\frac{2\pi na}{\lambda}\right)} \right] \right]^{-1} \tag{26}$$

where for cylindrical geometry $\alpha_n = 4\pi M(T/a)(2\pi na/\lambda)^2 I_0(2\pi na/\lambda) \cdot K_0(2\pi na/\lambda)$. The field is applied by a loop (of radius d) around the cylindrical film (of radius a), and h_n, h_n' are the Fourier coefficients of the field at the surface of the film and at the keeper (radius A), respectively. The axial field from a circular loop of radius d, at distance a from the axis and x from the plane of the loop, is given by[14,15]

$$H(x, a) = CI\left[K(k) + \frac{d^2 - a^2 - x^2}{(d-a)^2 + x^2} E(k) \right] / [(a+d)^2 + x^2]^{\frac{1}{2}},$$

where K and E are complete elliptic integrals of the first and second kinds, respectively, and $k^2 = 4da/[(a+d)^2 + x^2]$.

It can be noted that the effect of the keeper is to modify the applied field and to reduce the demagnetizing field. Fig. 17 shows a practical approximation to such a keeper geometry. Fig. 18 shows a plot of axial magnetization component in a 1μm thick permalloy film with H_K = 3.0 Oe plated on a 5.2 mil diameter wire, subject to the field from a one turn circular loop of diameter 7.5 mils carrying a current 0.3 amps.

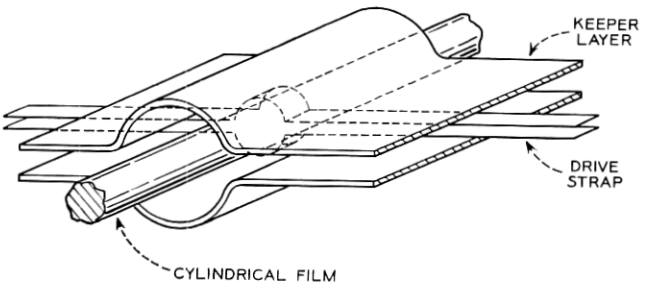

Fig. 17 — A possible practical approximation to a cylindrical keeper geometry.

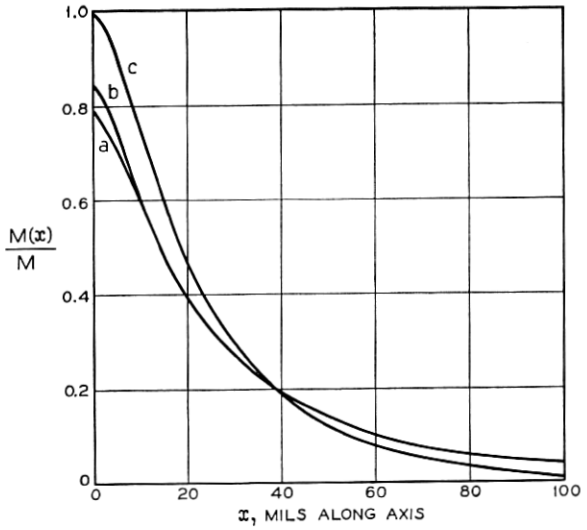

Fig. 18 — Effect of a cylindrical keeper layer on the axial magnetization distribution in a cylindrical film of thickness 1.0μm, $H_K = 3.0$ oe, diameter 5.2 mils. Field is applied by a one turn loop of radius 7.5 mils. Keeper radius is taken to be 10 mils. Curve a shows the distribution with no keeper present, curve b shows the effect of the keeper in modifying the applied field, and curve c shows the final result when field modification and flux closure are taken into account.

The keeper radius is taken to be 10 mils. Curve a shows the distribution with no keeper present, b shows the effect of field modification alone when a keeper cylinder of diameter 20 mils is in place, and c shows the final result when field modification and flux return are taken into account.

IX. NONUNIFORM HARD DIRECTION FIELD IN PRESENCE OF EASY DIRECTION BIAS FIELD

In this case the torque equation has to be modified to include the easy direction field $H_E(x)$, then

$$2K \sin \theta(x) \cos \theta(x) = M(H(x) - H_m(x)) \cos \theta(x) - MH_E(x) \sin \theta(x). \quad (27)$$

Providing $\cos \theta \neq 0$, we may write,

$$H_K \sin \theta(x) = H(x) - H_m(x) - H_E(x) \tan \theta(x), \quad (28)$$

where $H_K = 2K/M$ and it is assumed that H_E is parallel to the easy direction component of magnetization. It is convenient to represent $H_E(x) \tan \theta(x)$ by a series

$$H_E(x) \tan \theta(x) = \sum_{n=0}^{N} d_n \cos 2\pi n x/\pi.$$

Substituting into the torque equation (28), and gathering coefficients, we have

$$(H_K + \alpha_n)m_n = h_n - d_n, \qquad n = 0, 1, 2, \cdots, N.$$

The coefficients d_n are now complicated functions of the m_n's and this equation cannot be solved directly. Instead we use an iterative procedure as follows: $H(x)$ is given a peak value insufficient to produce saturation in the case $H_E = 0$ and then successive approximations are found for the m_n coefficients. In the first approximation we take

$$m_n = \frac{h_n}{H_K + \alpha_n}.$$

$\tan \theta(x)$ may now be found from $\sin \theta(x) = M(x)/M$, and the Fourier coefficients d_n of the product $H_E(x) \tan \theta(x)$, may be obtained. In the next approximation, we take

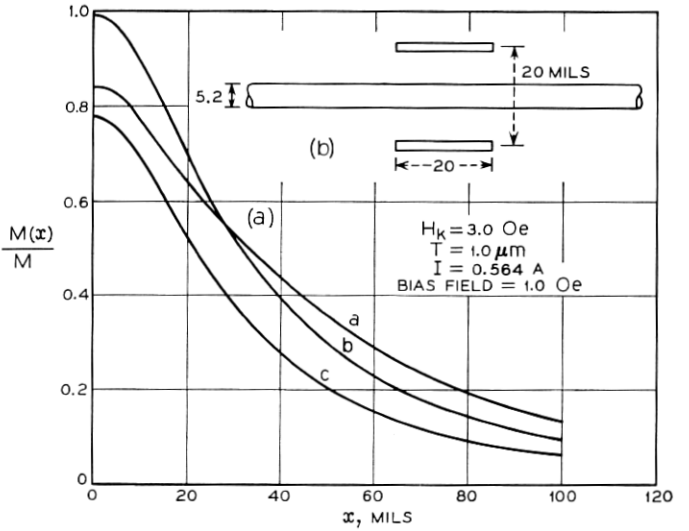

Fig. 19 — (a) Axial magnetization component for a cylindrical film with uniform easy direction bias field of 1.0 oe. The nonuniform hard direction field is applied by the drive strap arrangement shown in (b). In curve a, the bias field aids the rotation of magnetization for large x. A reverse domain is assumed to have been written into a width 20 mils, for $x < 10$ mils therefore the bias field opposes the rotation of magnetization. Curve b corresponds to zero bias field. Curve c corresponds to a reversal of bias field where it is assumed that the reversed region has been erased.

$$m_n = \frac{h_n - d_n}{H_K + \alpha_n}.$$

We now find, as before, new coefficients d_n ; hence, new coefficients m_n , until the m_n coefficients change by less than, say 5 percent per iteration. The curves for $H(x)$ and $M(x)$ are then plotted. The whole procedure may be repeated as necessary. The bias field may be a constant H_E or be a step function changing from H_E to $-H_E$ at some location $x = R$. The step function corresponds to the case of a domain wall being present at $x = R$. The use of the step function provides a formal way of treating the modification to the torque equation, due to H_E and the easy component of **M** being parallel for $x < R$, and antiparallel for $x > R$.

It is to be noted that the torque balance becomes unstable for certain combinations of applied fields. The critical fields are related by $[H(x) - H_m(x)]^{\frac{2}{3}} + H_E^{\frac{2}{3}} = H_K^{\frac{2}{3}}$, where it is assumed that H_E is antiparallel to the easy direction component of M. This limitation does not apply when H_E and the easy direction component of **M** are parallel.

Fig. 19 shows a typical axial magnetization distribution for a cylindrical film, and corresponds to the procedure of "writing" into a region of film. A current in the plated wire produces a uniform easy direction bias field of 1.0 oe and an external drive strap produces a nonuniform hard direction field. The greater spread of the curve *a* compared with the zero bias field distribution [shown by curve b] is due to the bias field lowering the effective anisotropy to $H_K - H_E$ for rotations less than about 40°. The attempt to "erase" by reversing the bias field, curve c, raises the apparent anisotropy to $H_K + H_E$ over much of the curve, and hence the film response is generally reduced. In curve c it is assumed that the reversed region has been erased. It will be appreciated that the present calculation assumes at the outset that a domain wall has some given location. The resulting distribution must then be inspected to decide whether the location chosen was appropriate or even stable under the applied field. In a practical case, wall location is affected by additional factors such as dispersion and creep, and is not discussed further here. Experiments on flat films show that the reversed region is not totally erased by simple reversal of bias field. Fig. 20(a) is a Kerr effect picture showing a reverse domain of width 20 mils, written in by a bias field of 1 Oe and a peak drive field of 5.0 Oe (11 mil strap, 10 mils from film). Fig. 20(b), shows the result of reapplying the fields with reversed bias. Fig. 20(c) shows the result of first demagnetizing the film into a fine domain structure, the width of the domain established is now much wider. In this case, the effect of the bias field changing the

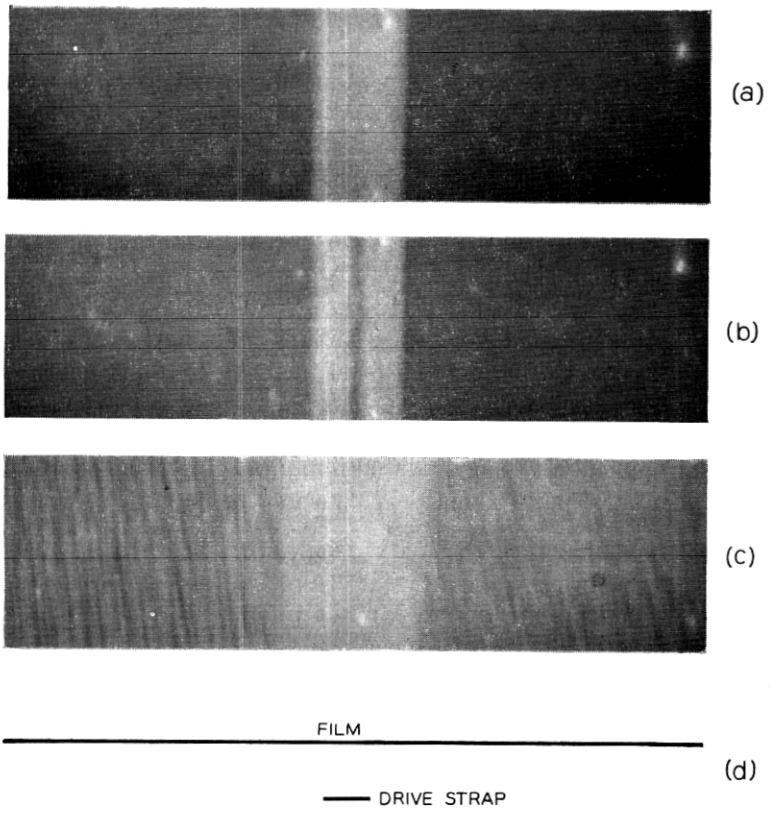

Fig. 20 — (a) Kerr effect picture showing reversed domain (light) in a flat film written in by an 11 mil drive strap situated 10 mils beneath the film. (b) When bias field is reversed, the domain is not completely erased. (c) Width of domain written after first demagnetizing film with a large uniform hard axis field. (d) Shows the drive strap arrangement to the same scale.

apparent anisotropy is much reduced, but the film now has an appreciable remanent state; hence, significant hard direction local demagnetizing fields exist in addition to the field introduced by the effect of the external fields. The relevance of such considerations to domain wall creep processes, under practical operating conditions, warrants further study but is not pursued here.

X. CONCLUSION

Demagnetizing fields play an important role in the operation of many thin magnetic film devices. The requirement of high packing density as in a memory, leads to strong localization of induced changes

in magnetization, and to correspondingly large demagnetizing fields and drive currents.

In an open flux structure attempts to confine magnetization changes by using segmented films or high anisotropy buffer regions are successful only at the expense of a considerable increase in drive field requirement. To some extent flux keeper layers may be used to modify applied fields and to permit partial flux closure, with in consequence, both a lowering of drive currents and a reduced spread in induced magnetization component.

The method of calculation given here permits a detailed examination to be made of the effectiveness of such procedures, and has been applied to a variety of thin film demagnetizing field problems. Kerr effect probe measurements[6] are in good agreement with calculation although relatively little data is at present available. The results have particular applicability to cylindrical film problems, where axial variation of field or properties is of primary concern.

XI. ACKNOWLEDGMENT

Acknowledgments are due to Mrs. L. Calamia for valuable assistance with the computer programs.

REFERENCES

1. Leaver, K. D. and Prutton, M., The Effect of Applied Field Inhomogeneity on the Reversal Behavior of Thin Magnetic Films, J. Elect. Control, *15*, 1963, pp. 173–181.
2. Edwards, J. G., Apparent Anisotropy Field of Continuous Magnetic Films Subjected to Inhomogeneous Drive Fields, Nature, *7*, 1963, pp. 130–134.
3. Rosenberg, R., unpublished work.
4. Kump, H. J. and Greene, T. G., Magnetization of Uniaxial Cylindrical Thin Films, IBM J., *7*, 1963, p. 130.
5. Kump, H. J., Demagnetization of Flat Unixial Thin Films Under Hard Direction Drive, IBM J., *9*, 1965, p. 118.
6. Dove, D. B. and Long, T. R., Magnetization Distribution in Flat and Cylindrical Films Subject to Nonuniform Hard Direction Fields, IEEE Trans. on Magnetics, *2*, 1966, pp. 194–197.
7. Gradshteyn, I. S. and Ryzhik, I. M., *Tables of Integrals, Series and Products*, Editor, A. Jeffrey, Academic Press, New York, 1965.
8. Erdélyi, A., Editor, *Bateman Manuscript Project*, McGraw-Hill Book Co., New York, 1954.
9. Osborne, J., Demagnetizing Factors of the General Ellipsoid, Phys. Rev., *67*, 1945, p. 351–357.
10. Dove, D. B., Anisotropy Magnitude Dispersion in Thin Films, Electronics Letters, *2*, 1966, pp. 15–16.
11. Combs, C. A. and Wujek, J. H., On the Static Magnetic Field Associated with a Thin Film Ferromagnetic Slab, J. Franklin Institute, *277*, 1964, pp. 305–312.
12. Pohm, A. V., Heller, L. G., and Smay, T. A., Adjacent Element Coupling in Continuous Film Memories, IEEE Trans. on Magnetics, *2*, 1966, pp. 512–515.

13. Feltl, H. and Harloff, H. J., Flux Keepers in Magnetic Thin Film Memories, IEEE Trans. on Magnetics, *2*, 1966, pp. 516–520.
14. Stratton, J. A., *Electromagnetic Theory,* McGraw-Hill Book Co., New York, p. 263.
15. Nagaoko, N., Magnetic Field of Circular Currents, Phil. Mag. Series 6, *41*, 1920, pp. 377–388.